JOURNAL

OF THE AMERICAN CHEMICAL SOCIETY

VOLUME 105, NUMBER 8 APRIL 20, 1983

Assignment of Hyperfine-Shifted Resonances in Low-Spin Forms of Cytochrome *c* Peroxidase by Reconstitutions with Deuterated Hemins

James D. Satterlee,*[1a] James E. Erman,[1b] Gerd N. LaMar,[1c] Kevin M. Smith,[1c] and Kevin C. Langry[1c]

Contribution from the Departments of Chemistry, University of New Mexico, Albuquerque, New Mexico 87131, Northern Illinois University, DeKalb, Illinois 60115, and University of California, Davis, California 95616. *Received July 19, 1982*

Abstract: Proton magnetic resonance assignments of protons from peripheral heme substituents have been carried out for two low-spin forms of cytochrome *c* peroxidase: CcP-CN and CcP-N_3. The assignments were made by reconstituting CcP with six specifically deuterated protohemin IX derivatives. The results indicate that the pattern of unpaired π spin-density delocalization is consistent with an interpretation whereby the source of the rhombic perturbation is the orientation of the proximal histidine's imidazole plane. However, we also present evidence that a specific interaction between pyrrole II and tryptophan 51 affects the observed shift pattern, thereby contributing to the rhombic perturbation.

Cytochrome *c* peroxidase (EC 1.11.1.5; ferrocytochrome *c* oxidoreductase; CcP) is a soluble, ferric heme enzyme associated with yeast mitochondria.[2,3] Its role in nature is to catalyze the hydrogen peroxide oxidation of ferrocytochrome *c*, and during this process it functions via ligand binding reactions as well as redox catalysis. Like most b-type heme proteins, CcP exhibits distinct magnetic and ligation states.[4,5] The native, resting enzyme has been shown to be predominantly high spin[2] and six-coordinate[6,7] with a water molecule occupying the sixth axial position. CcP readily binds small, anionic ligands, with the resulting complexes yielding magnetic and spectroscopic data characteristic of a range of intermediate to low spin states.[2,8-14] In fact, a six-coordinate low-spin ferryl form[15] has been identified as one of the active intermediates of the enzymic cycle, Ccp–I (compound I, ES complex). CcP–I most likely originates from initial, transient coordination of hydrogen peroxide to the heme followed by one or more rapid oxidation steps.[16]

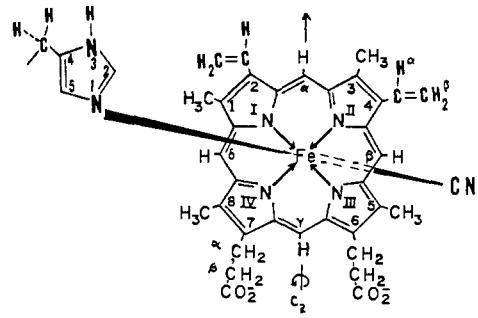

I

By virtue of the paramagnetism that characterizes all of the ligation states of CcP, the hyperfine proton NMR spectrum can be valuable for quantitating the dynamics of ligand binding[17] and detecting molecular-level fluctuations within the active site.[18,19] For CcP and other heme proteins, NMR has identified heme-centered asymmetry and defined the mechanism by which it is established.[20-25] Until now the greatest impediment for inter-

(1) (a) University of New Mexico. (b) Northern Illinois University. (c) University of California.
(2) Yonetani, T. *Enzymes* **1976**, *13c*, 345–361.
(3) Hewson, W. D.; Hager, L. P. *Porphyrins* **1979**, *7B*, 295–332.
(4) Bearden, A. J.; Dunham, W. R. *Struct. Bonding (Berlin)* **1970**, *8*, 1–52.
(5) LaMar, G. N.; Walker, F. A. *Porphyrins* **1979**, *6B*, 61–157.
(6) Poulos, T. L.; Freer, S. T.; Alden, R. A.; Edwards, S. L.; Skoglund, U.; Takio, K.; Eriksson, B.; Xuong, N.; Yonetani, T.; Kraut, J. *J. Biol. Chem.* **1980**, *255*, 575–580.
(7) Satterlee, J. D.; Erman, J. E.; LaMar, G. N.; Smith, K. M.; Langry, K. C. *Biochim. Biophys. Acta*, in press.
(8) Yonetani, T.; Schleyer, H. *J. Biol. Chem.* **1967**, *242*, 3926–3933.
(9) Wittenberg, B. A.; Kampa, L.; Wittenberg, J. B.; Blumberg, W. E.; Peisach, J. *J. Biol. Chem.* **1968**, *243*, 1863–1870.
(10) Wittenberg, B. A.; Kampa, L.; Wittenberg, J. B.; Blumberg, W. E.; Peisach, J. *J. Biol. Chem.* **1968**, *243*, 1871–1876.
(11) Yonetani, T.; Schleyer, H. *J. Biol. Chem.* **1967**, *242*, 3919–3925.
(12) Lang, G.; Asakura, T.; Yonetani, T. *J. Phys. C* **1969**, *2*, 2246–2255.
(13) Erman, J. E. *Biochemistry* **1974**, *13*, 34–38.
(14) Erman, J. E. *Biochemistry* **1974**, *13*, 39–43.
(15) Coulson, A. F. W.; Yonetani, T. *Biochemistry* **1975**, *14*, 2389–2395.
(16) Poulos, T. L.; Kraut, J. *J. Biol. Chem.* **1980**, *255*, 8199–8205.
(17) Satterlee, J. D.; LaMar, G. N.; Frye, J. S. *J. Am. Chem. Soc.* **1976**, *98*, 7275–7281.
(18) LaMar, G. N.; Overkamp, M.; Sick, H.; Gersonde, K. *Biochemistry* **1978**, *17*, 352–362.
(19) LaMar, G. N.; Viscio, D. B.; Gersonde, K.; Sick, H. *Biochemistry* **1978**, *17*, 361–367.
(20) LaMar, G. N. In "Biological Applications of Magnetic Resonance"; Shulman, R. G., Ed.; Academic Press: New York, 1979; pp 305–343.

0002-7863/83/1505-2099$01.50/0

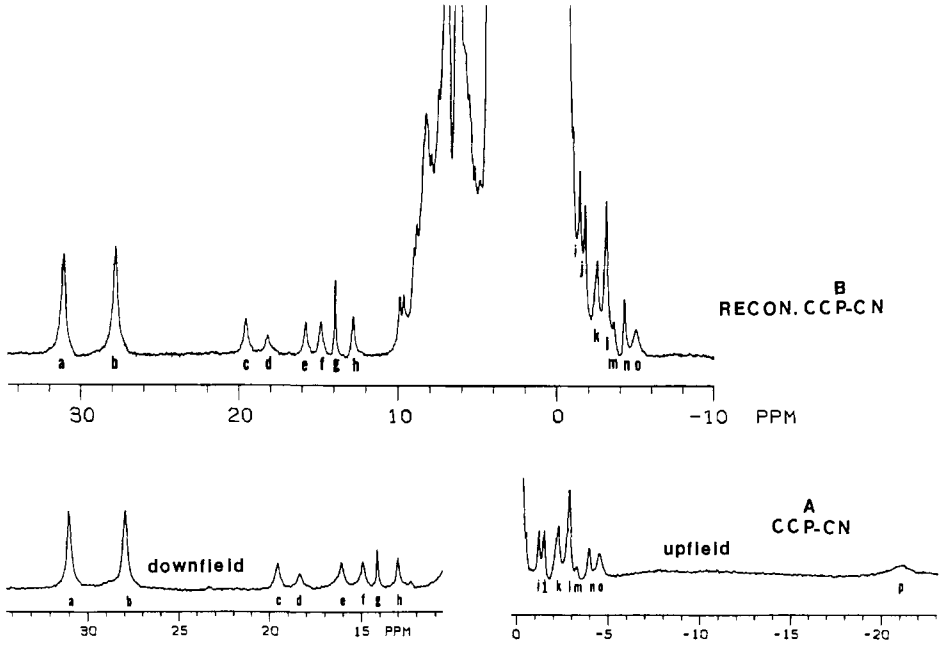

Figure 1. Proton NMR spectra of heme proteins used in this study: (A) native CcP-CN; (B) protohemin-reconstituted CcP-CN, 24 °C, pH 7.0–7.5, 0.1 M KNO_3. This figure indicates peak identification and reveals that no heterogeneity exists in native or reconstituted samples. Peak p (A) occurs in both samples and all other reconstituted spectra even though it is not shown in B. Note different scaling for A and B.

preting much of the existing proton NMR data on CcP[26] and other heme proteins has been an inability to unambiguously assign the resolved hyperfine resonances. Development of synthetic techniques[27] for introducing deuterium enrichment into peripheral substituents of protohemin IX (I), with subsequent reconstitution into an apoprotein, offered the best solution to this problem and has lead to several significant results.[7,20-22,24,25,28-30]

In this work we present the results of proton hyperfine resonance assignments for CcP-N_3 and CcP-CN employing the method of incorporating specifically deuterated hemins into apo-CcP. These results are meant to supplement our previous assignments for the CcP high-spin forms.[7] This effort was undertaken to facilitate correct and detailed interpretation of a large body of existing CcP data.[26] In addition, these assignments allow comparisons to be made with similar data for horseradish peroxidase[22,29] (EC 1.11.1.7; HRP), metmyoglobin,[21] and monomeric hemoglobins.[20] Such comparisons are important if molecular-level differences in solution-state heme crevice structure are to be delineated for different b-type heme protein functional classes.

Experimental Section

The isolation, purification, and reconstitution of CcP has been previously described, as has the hemin nomenclature that will be used.[7] One additional hemin was available for this study. We refer to the hemin in which the four methylene protons adjacent to the propionic acid carboxyl group are deuterated as [6,6,7,7-$^2H_4$]hemin. Azide-ligated forms of CcP were established by adding a 25-fold mole excess of potassium azide to the reconstituted CcP solutions. Following use, the azide samples were extensively dialyzed against 0.1 M KNO_3 in ^2H_2O solution (Merck 99.8%) to remove the azide ion. Potassium cyanide in 1.1 mole excess was added, and the solutions were concentrated to their final volumes by ultrafiltration using an Amicon microultrafiltration cell. Throughout this entire procedure the solution pH was constantly monitored and regulated by addition of dilute ^2HCl so that the pH range was maintained between 7.0 and 7.5. Samples were ultimately unbuffered within this pH range in 0.1 M KNO_3.

Proton NMR spectra were recorded on Nicolet spectrometers operating at a variety of proton frequencies: 200 MHz (4.7 T), 360 MHz (8.45 T), and 470 MHz (11.0 T). The 360-MHz spectra were obtained at the University of California, Davis, NMR Facility, whereas 200- and 470-MHz spectra were taken at the Purdue University Biochemical Magnetic Resonance Laboratory. Details of the NMR data accumulation are as before.[23,38]

Results and Discussion

General Spectral Characteristics. As with our assignments in the high-spin CcP forms,[7] it was necessary to determine whether reconstitution of apo-CcP with protohemin IX would lead to more than one set of reconstituted CcP-CN resonances, characteristic of heme-centered asymmetry.[23,39] Such is the case for reconstituted deuterohemin IX CcP-CN and CcP-N_3. Because the line widths for each of these are an order of magnitude smaller than

(21) LaMar, G. N.; Budd, D. L.; Viscio, D. B.; Smith, K. M. *Proc. Natl. Acad. Sci. U.S.A.* **1978**, *75*, 5755–5759.
(22) LaMar, G. N.; DeRopp, J. S.; Smith, K. M.; Langry, K. C. *J. Am. Chem. Soc.* **1980**, *102*, 4835–4836.
(23) Satterlee, J. D.; Erman, J. E. *J. Am. Chem. Soc.* **1981**, *103*, 199–200.
(24) Budd, D. L.; LaMar, G. N.; Langry, K. C.; Smith, K. M.; Nayyir-Mazhir, R. *J. Am. Chem. Soc.* **1979**, *101*, 6091–6096.
(25) LaMar, G. N.; Gersonde, K.; Sick, H.; Overkamp, M. *J. Biol. Chem.* **1980**, *255*, 66–70.
(26) Satterlee, J. D.; Erman, J. E. *Biochim. Biophys. Acta*, in press.
(27) Smith, K. M.; Eivarzl, F.; Langry, K. C.; De Alameida, J. A. P. B.; Kenner, G. W. *Bioorg. Chem.* **1979**, *8*, 485–495.
(28) LaMar, G. N.; Burns, P. D.; Jackson, J. T.; Smith, K. M.; Langry, K. C.; Strittmatter, P. *J. Biol. Chem.* **1981**, *256*, 6075–6079.
(29) DeRopp, J. S. Ph.D. Dissertation, University of California, Davis, 1981.
(30) Mayer, A.; Ogawa, S.; Shulman, R. G.; Yamane, T.; Cavaleiro, J. A. S.; Rocha Gonsalves, A. M. d'A.; Kenner, G. W.; Smith, K. M. *J. Mol Biol.* **1974**, *86*, 749–756.
(31) Morishima, I.; Ogawa, S.; Yonezawa, T. *Biochim. Biophys. Acta* **1978**, *537*, 293–303.
(32) Morishima, I.; Neya, S.; Inubushi, T.; Yonezawa, T.; Iizuka, T. *Biochim. Biophys. Acta* **1978**, *534*, 307–316.
(33) LaMar, G. N.; Budd, D. L.; Smith, K. M. *Biochim. Biophys. Acta* **1980**, *622*, 210–218.
(34) Shulman, R. G.; Glarum, S. H.; Karplus, M. *J. Mol. Biol.* **1971**, *57*, 93–115.
(35) Walker, F. A. *J. Am. Chem. Soc.* **1980**, *102*, 3254–3256.
(36) Poulos, T. L.; Freer, S. T.; Alden, R. A.; Xuong, N. H.; Edwards, S. L.; Hamlin, R. C.; Kraut, J. *J. Biol. Chem.* **1978**, *253*, 3730–3735.
(37) Satterlee, J. D.; Erman, J. E. *Arch. Biochem. Biophys.* **1980**, *202*, 608–616.
(38) Satterlee, J. D.; Erman, J. E. *J. Biol. Chem.* **1981**, *256*, 1091–1093.
(39) Keller, R.; Groudinsky, O.; Wuthrich, K. *Biochim. Biophys. Acta* **1976**, *427*, 497–511.
(40) Satterlee, J. D.; LaMar, G. N. *J. Am. Chem. Soc.* **1976**, *98*, 2804–2812.
(41) LaMar, G. N.; Viscio, D. B.; Smith, K. M.; Caughey, W. S.; Smith, M. L. *J. Am. Chem. Soc.* **1978**, *100*, 8085–8091.
(42) Welinder, K. G. *FEBS Lett.* **1976**, *72*, 19–23.
(43) Takio, K.; Titani, K.; Ericsson, L. H.; Yonetani, T. *Arch. Biochem. Biophys.* **1980**, *203*, 615–629.

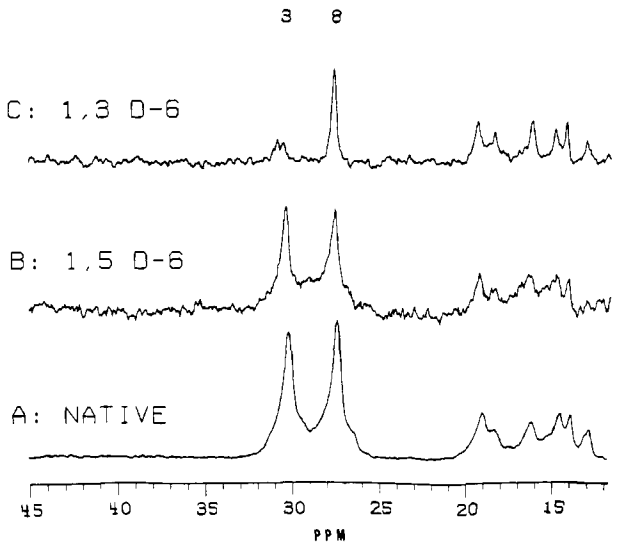

Figure 2. Assignment of hemin methyl protons by deuteration: (A) native CcP-CN; (B) CcP_2 reconstituted with [1,5-$^2H_6$]hemin; (C) CcP reconstituted with [1.3-$^2H_6$]hemin. Cyanide forms were established as described in the text. The enzyme was in 0.1 M KNO_3, pH 7–7.4, at 24 °C.

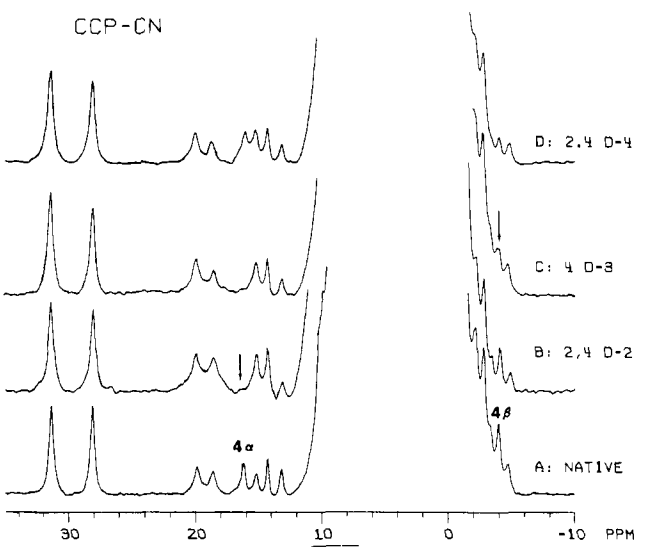

Figure 3. Assignment of hemin vinyl protons by deuteration in CcP-CN. Both upfield and downfield regions are shown in this figure, although upfield assignments are more distinct in Figure 4: (A) native CcP-CN; (B) α-vinyl's deuterated; (C) 4-vinyl group perdeuterated (both α and β protons); (D) β-vinyl protons deuterated. Conditions were as described in Figure 2.

those for the high-spin forms, even minor (5–10%) amounts of a second form, which would not have been detected in the (high spin) CcP or CcP-F spectra, could easily be identified in CcP-CN or CcP-N_3 spectra.

Figure 1 shows that compared to CcP-CN, protohemin-reconstituted CcP-CN gives no evidence of a second form. In Figure 1A the spectrum of CcP-CN generated from crystallized native CcP indicates that it is typical of spectra for the cyanide-ligated species of other b-type ferric heme proteins.[20-22] In deuterium oxide (^2H_2O) solution, the two large peaks that lie farthest downfield have relative intensities of three protons each (peaks a, b). These originate from two of the four hemin methyl groups (I). Further upfield, between 10 and 20 ppm, lie six (peaks c–h) resonances with relative intensities corresponding to one proton each. Upfield, between 0 and −6 ppm there are several resonances whose relative intensities correspond to one (peaks i–j, n–p) or two (peaks k, l) protons. One resonance (m) corresponds to an intensity less than one proton and is likely due to orientational heterogeneity of a protein group, as found for HRP.[44] The spectrum in Figure 1B is that of protohemin reconstituted CcP-CN and is identical with Figure 1A, with no additional minor peaks detectable.

Figure 6A shows a spectrum of CcP-N_3 generated from native CcP. As with CcP-CN, no peaks attributable to a second form are detected when protohemin-resonstituted CcP is used. It is considered unnecessarily redundant to indicate this with an additional spectral trace. In proton spectra of the downfield hyperfine region of CcP-N_3 (Figures 5 and 6), four larger resonances (peaks A–D) are resolved, which may be tentatively assigned to the four hemin methyl groups. Variable-temperature studies have shown that peak E results from the overlap of several single-proton resonances at the pH and temperature of Figures 5 and 6. In addition, several overlapping single-proton resonances occur between 10 to 25 ppm and 0 to −10 ppm. This spectrum is also grossly typical of proton spectra obtained for other azide-ligated ferric heme proteins.[31,32]

CcP-CN Resonance Assignments. Two of the four hemin methyl groups are resolved in the hyperfine region (peaks a, b), and their assignments are shown in Figure 2. In Figure 2A a downfield hyperfine spectrum of native CcP-CN is shown.

In Figure 2B the spectrum that results from reconstitution of apo-CcP with [1,5-$^2H_6$]hemin is shown. Relative to the neighboring single-proton resonances (peaks c–h), the relative intensities of the two methyl resonances remain unchanged, indicating that neither of the observed resonances correspond to methyls 1 or 5.

Figure 2C shows the downfield hyperfine spectrum of [1,3-$^2H_6$]hemin-reconstituted CcP-CN. In contrast to Figures 2A, and 2B, the methyl resonance farthest downfield has experienced a dramatic intensity reduction relative to surrounding resonances. Consequently, it is assigned to methyl 3. The peak (b) that remains unchanged throughout is assigned to methyl 8, the only methyl group that has not been deuterated.

Single-proton assignments are shown in Figures 3 and 4. The downfield region of the spectrum is depicted in Figure 3. The native spectrum in Figure 3A is a different sample from that used for the methyl assignments (Figure 2). Between 12 and 22 ppm, six single-proton resonances occur (c–h). Reconstituting with [2,4-$^2H_2$]hemin yields spectrum 3B, in which the peak near 16.0 ppm (e) is absent. In spectrum 3C, a reconstitution with [4-$^2H_3$]hemin in which the 4-vinyl group is completely deuterated, this peak remains missing, indicating that it is assignable to the 4-position α-vinyl proton. Reconstituting with [2,4-$^2H_4$]hemin, in which only the β-vinyl protons are deuterated, yields a downfield hyperfine spectrum identical with native CcP-CN, confirming this assignment.

Assignment of the resonances that lie upfield from DSS is shown in Figure 4. Again, Figure 4A corresponds to CcP-CN generated from native enzyme. Figure 4, B, C, and D, shows respectively the reconstitutions with [2,4-$^2H_4$]hemin, [2,4-$^2H_2$]hemin, and [4-$^2H_3$]hemin. Only peak n shows a relative reduced intensity in Figures 4B and 4D compared to Figures 4A and C and is thereby unambiguously assigned to a β-vinyl proton at position 4. This resonance does not completely disappear due to incomplete deuteration at the 4β-position. An additional broad resonance (see Figure 1) labeled p lies further upfield, near −20 ppm. Its line width and position coincide with that found for the 2-position proton of an axially coordinated imidazole in model complexes[5,42] and proteins.[39] Indeed, elsewhere[45] we have presented evidence for making this assignment to the proximal 2-H in CcP-CN. This, along with the other shifts and assignments, is summarized in Table I.

CcP-N_3 Resonance Assignments. Figure 5 shows the assignment of hemin methyl proton resonances for CcP-N_3 in the region between 20 and 50 ppm downfield. Five peaks present themselves in this region (peaks A–E), and the relative areas of each ranges

(44) LaMar, G. N.; DeRopp, J. S.; Smith, K. M.; Langry, K. C. *J. Biol. Chem.* **1980**, *255*, 6646–6651.

(45) LaMar, G. N.; DeRopp, J. S.; Chacko, V. P.; Satterlee, J. D.; Erman, J. E. *Biochim. Biophys. Acta* **1982**, *708*, 317–325.

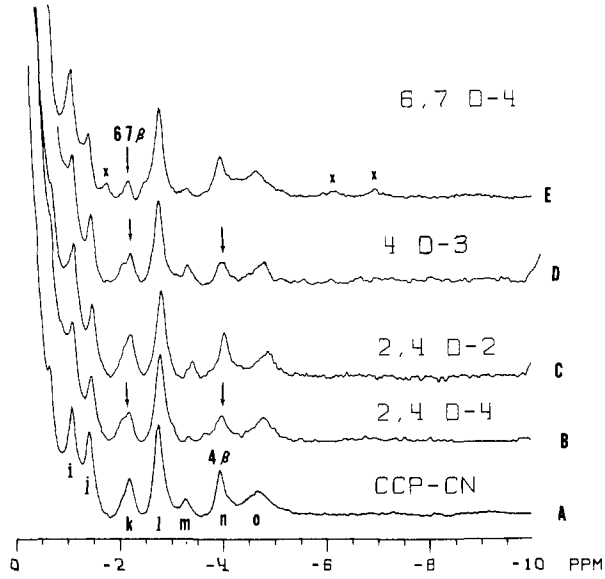

Figure 4. Assignment of upfield single protons via deuteration. Two resonances are assigned, a-β-vinyl and a 6- or 7-position β-propionic acid methylene proton: (A) native CcP-CN; (B) [2,4-$^2H_4$]hemin-CcP-CN; (C) [2,4-$^2H_2$]hemin-CcP-CN; (D) [4-$^2H_3$]hemin-CcP-CN; (E) [6,7β-$^2H_4$]hemin-CcP-CN. Arrows indicate peaks that show decreased intensity, reflecting deuteration.

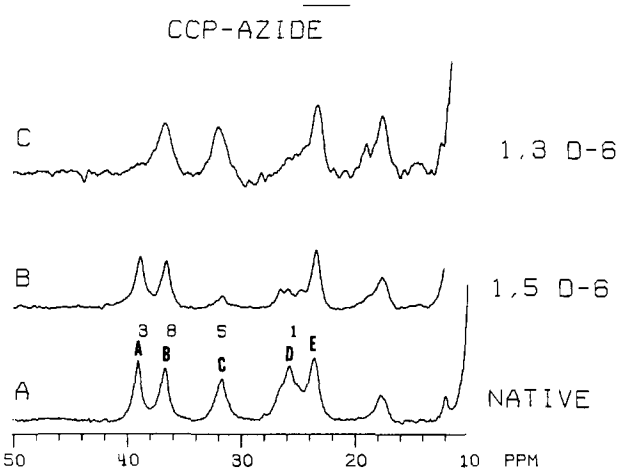

Figure 5. Assignment of hemin methyl resonances in CcP-N_3 by deuteration: (A) native CcP-N_3; (B) [1,5-$^2H_6$]hemin-CcP-N_3; (C) [1,3-$^2H_6$]hemin-CcP-N_3. The enzyme was in 0.1 M KNO_3, pH 7.4, 24 °C.

between three and five protons due to the coincidence of one or more resonances. By reconstituting with deuterated hemins, as before, and looking for relative intensity decreases, one can assign the methyls in the order 3 > 8 > 5 > 1. Figure 5A shows the native CcP-N_3 spectrum. Upon reconstitution with [1,5-$^2H_6$]-hemin, peaks C and D, at 31.9 and 25.8 ppm, display reduced intensity (Figure 5B). When [1,3-$^2H_6$]hemin is used, peaks at 38.9 (A) and 25.8 ppm (D) disappear, leaving a detectable amount of residual proton intensity that is due either to incomplete methyl group deuteration or overlap of the methyls with single protons or both. The assignments are indicated in Figure 5 and Table I.

Single-proton resonance assignments are shown in Figure 6. The native CcP-N_3 spectrum is presented in Figure 6A. In Figure 6B, the spectrum that results from incorporation of [2,4-$^2H_4$]hemin into apo-CcP shows that only the two resolved upfield resonances (G, H) at −2.9 and −5.6 ppm display decreased intensities, indicating their assignment to vinyl β-protons. Both relative intensities are seen to return to normal values in subsequent spectra, so these are assigned to the vinyl at position 2. Figure 5C is a spectrum of [4-$^2H_3$]hemin-CcP-N_3 and Figure 5D is a spectrum of the [2,4-$^2H_2$]hemin reconstituted enzyme. Noteworthy in these

Table I. Hyperfine Resonance Assignments in Low-Spin CcP Forms[a]

	shift			
	CcP-CN (22 °C)		CcP-N_3 (25 °C)	
assignment	observed	hyperfine[b]	observed	hyperfine
A. methyls				
3	31.2	27.6	38.9	35.3
8	27.3	23.7	36.8	33.2
5			31.9	28.3
1			25.8	22.2
B. vinyls				
2-α			17.6	9.0
4-α	15.9	7.3	23.8 (?)	15.2
2-β			−2.9	−9.2
			−5.6	−11.9
4-β	−4.0	−10.3		
	−2.2 (?)	−8.5 (?)		
C. propionic acid				
6- or 7-	−2.2	−5.6		
D. Proximal histidine	−21			

[a] Shifts in ppm, referenced to residual H_2O, reported relative to external DSS. [b] Hyperfine or isotropic shifts obtained by referencing observed shifts to their corresponding diamagnetic position, see ref 41, Table I.

two spectra is the dramatic intensity decrease of the resonance at 17.6 ppm in Figure 6D, whereas its intensity is retained in Figure 6C. This indicates its assignment as an α-vinyl proton at position 2. Another single-proton assignment is suggested from these spectra, as well, when one notices the reduced relative intensity of resonance E (23.8 ppm) in Figure 5, C and D, compared to Figure 5, A and B. As a result we tentatively suggest that the 23.8 ppm group of overlapping resonances contains the 4-vinyl α-proton.

Interpretation of the Hyperfine Shift Pattern. Assignment of the hyperfine resonances in CcP-CN and CcP-N_3 can result in conclusions about the interactions between the hemin and the protein. It has been demonstrated for substituted iron porphyrins[21] that the pattern of hemin proton resonances is altered upon reconstitution into a protein such as metmyoglobin.[33] This change has been attributed to a low-symmetry perturbation within the protein, which has two possible origins: (a) the rotational position of the proximal histidine imidazole ring,[34,35] and (b) asymmetric interaction of the protein with the hemin periphery[18,33,41] or both.

From the resonance positions in Table II, collected for CcP, HRP, and metmyoglobin, certain trends are evident in the hyperfine resonance pattern. These may be interpreted by noting that although these protein complexes exhibit magnetic anisotropy, work on similar low-spin hemin models has indicated that the magnitude of the dipolar shift in such systems is too small to alter the relative methyl ordering.[41] The conclusion reached is that the observed hyperfine resonances that are to be discussed here are dominated by the contact shift and are a result of metal–ligand covalency. In low-spin ferric molecules with local site symmetry C_4, the partially filled d_{xz}, d_{yz} iron orbitals may participate with the porphyrin 3e π-filled molecular orbital in Por → Fe π spin-density transfer, thereby distributing unpaired π-type spin density around the heme ring and establishing the characteristic hyperfine shift pattern.[5,20,41] Modulation of this unpaired distribution may occur through the rotational position of the proximal imidazole plane relative to the heme plane, which regulates the extent of interaction of the imidazole π system with the hemin π system,[5,34,35] or through peripheral hemin–protein interactions that may direct spin density via donor/acceptor and steric forces.[41]

Because both effects have been shown to be capable, in principle, of accounting for the ordering of hemin methyl proton resonances, both mechanisms must be considered. In fact, for hemin models both mechanisms have, to-date, explicitly demonstrated the ca-

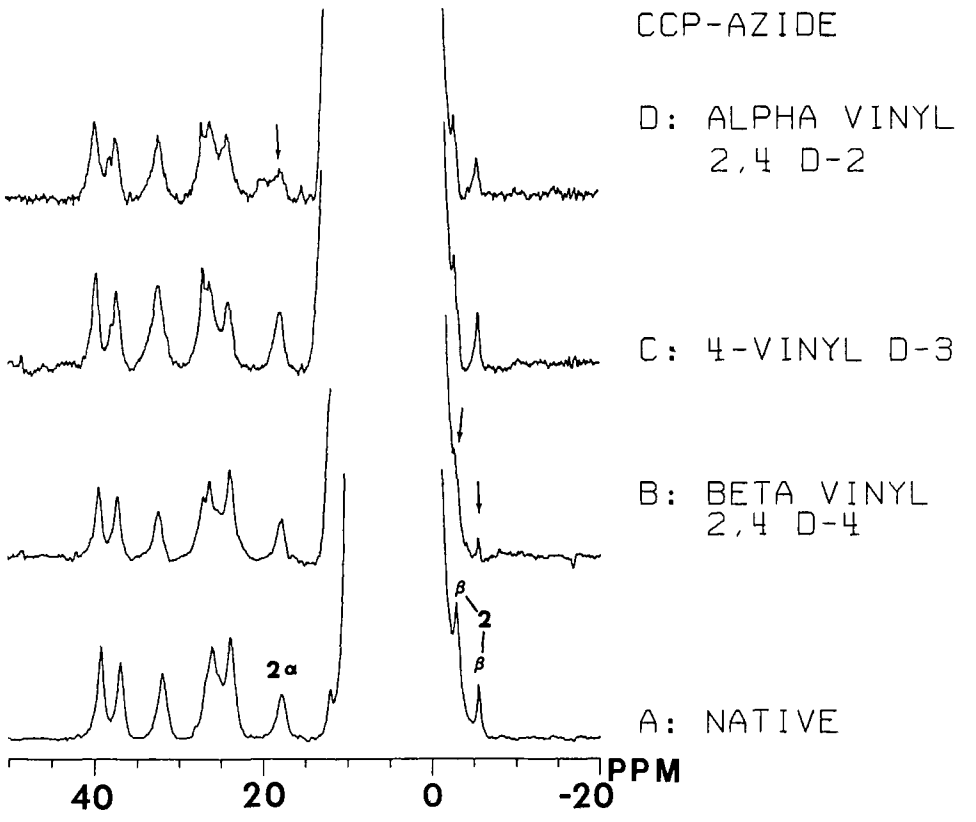

Figure 6. Assignment of single proton resonances in CcP-N_3 by reconstitution with deuterated hemins: (A) native CcP-N_3; (B) [2,4-$^2H_4$]hemin–CcP-N_3; (C) [4-$^2H_3$]hemin–CcP-N_3; (D) [2,4-$^2H_2$]hemin–CcP-N_3. Conditions are the same as described in Figure 5. Arrows indicate peaks displaying decreased intensity as a result of deuteration.

Table II. Methyl Hyperfine Resonance Positions for Ferric Heme Proteins

	hemin methyls				ref
A. azide					
Mb-N_3					
rel order	5	1	8	3	
obsd shift[a] (25 °C)	31.6	26.2	24.4	*b*	33
pyrrole[c]	(III	I)	(IV	II)	
CcP-N_3					
rel order	3	8	5	1	
obsd shift (25 °C)	38.9	36.8	31.9	25.8	this work
pyrrole	(II	IV)	(III	I)	
B. cyanide					
Mb-CN					
rel order	5	1	8	3	
obsd shift (25 °C)	27.4	18.7	13.0	*b*	33
pyrrole	III	I	IV	II	
CcP-CN					
rel order	3	8			this work
obsd shift (22 °C)	31.2	27.3	*b*	*b*	
pyrrole	II	IV	(III, I)		
HRP-CN					
rel order	8	3	*b*	*b*	
obsd shift (35 °C)	29.8	24.9			29
pyrrole	IV	II	(III, I)		

[a] In ppm. [b] Resonances not resolved. [c] For definition refer to I or Figure 7.

pability to mimic the spread of resonances observed in heme proteins.[41,46]

In the azide forms the data can be simply interpreted by noting that the methyl resonances separate into pairs corresponding to substituents on trans (opposite) pyrroles. In metmyoglobin-N_3,

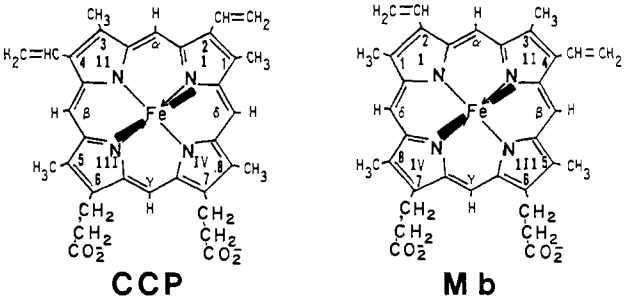

Figure 7. Comparison of the proximal histidine (imidazole) plane projection onto the hemin for CcP and Mb. This view is along the proximal histidine–Fe bond and was formulated from the published crystal structures for each, as described in the text. Note the interchange of pyrroles I,II and III,IV in the two structures. This is equivalent to a 180° rotation about the α–γ (meso) axis.

pyrroles I and III (methyls 5 and 1) exhibit further downfield shifts, indicating greater delocalization of unpaired spin density, than pyrroles II and IV (methyls 3 and 8). The order is precisely reversed in CcP-N_3, where pyrroles II and IV receive relatively more spin density compared to pyrroles I and III. The CcP-N_3 resonance order shows that methyls 3 and 8 exhibit more downfield shifts compared to methyls 5 and 1. The 180° rotational isomerism about the meso α–γ axis (Figure 7) observed in the CcP crystal structure, compared to myoglobin,[6] accounts for the pairwise interchange of spin delocalization between trans pyrroles. When compared with the crystallographically determined orientation of the proximal histidine's imidazole plane (Figure 7), this data indicated that the observed shift pattern in both CcP-N_3 and met-Mb-N_3 is consistent with an interpretation that attributes the rhombic perturbation to the orientation of the imidazole plane.

A similar argument can be made for the data in Table IIB. Again the CcP-CN data differs from metmyoglobin-CN in a trans pairwise manner, which can be rationalized by the 180° rotation about the α–γ meso axis relative to a fixed proximal imidazole

(46) Traylor, T. G.; Berzinis, A. P. *J. Am. Chem. Soc.* **1980**, *102*, 2844–2846.

plane (Figure 7). At minimum, this data can be accounted for by the imidazole orientation. Notably, the data of Table II indicate that HRP-CN exhibits a resonance pattern similar to CcP in that pyrroles II and IV (methyl pair 8 and 3) exhibit larger shifts than pyrroles I and III (methyl pair 5 and 1). These data imply that the heme orientation in HRP, relative to a fixed proximal histidine-iron bond, is similar to that in CcP.[47] We conclude that HRP also will exhibit a hemin orientation reversed by 180° about the α-γ meso axis when compared to metmyoglobin.

Whether, and to what extent, peripheral hemin-protein contact may influence the methyl shift pattern in low-spin heme proteins remains to be evaluated. There is evidence from the data of Table II, in fact, that heme-protein peripheral contacts constitute at least a minor part of the rhombic perturbation in these CcP forms. We deduce this by comparing the 3,8-shifts in both CcP and HRP as shown in Figure 7. At 35 °C the most downfield resonances are HRP (8) and CcP (3). The more upfield pair are HRP(3) and CcP(8). A reasonable source for this reversal of trans pyrrole methyl shifts between CcP and HRP lies in different heme-protein peripheral contacts at the trans pyrroles (II,IV). Crystal structure data has only been reported for CcP,[6,16] and it indicates that Trp-51, a critical residue to the proposed peroxidase catalysis mechanism[16,36] lies above pyrrole II. Primary sequence studies of HRP[42,43] indicate a high degree of homology in the B helix of CcP, which forms the distal side of the heme pocket. However, in place of Trp-51, the HRP sequence places a phenylalanine. In view of the greater charge-donating ability of tryptophan compared to phenylalanine, the inversion of the 3,8-methyl resonance ordering that is observed here can be understood by assuming significant peripheral contact between the position-51 residue and the hemin. Donation of charge density to pyrrole II from the tryptophan enhances the Por → Fe π donation by pyrrole II, thereby shifting the 3-CH_3 further downfield and, hence, inverting the methyl ordering in CcP relative to HRP. In support of this possibility we note that the mean 3,8-methyl resonance position in CcP (28.2 ppm at 35 °C) is much larger than the mean 3,8-shift in HRP (27.3 ppm at 35 °C). This shift pattern indicates that the porphyrin 3e π-orbital which includes pyrroles II and IV contains relatively greater unpaired spin density in CcP than does the same orbital in HRP.

(47) LaMar, G. N.; deRopp, J. S.; Smith, K. M.; Langry, K. C., unpublished data.

Summary

Hemin methyl, vinyl, and propionic acid methylene protons have been assigned for CcP-CN and CcP-N_3 by reconstitution with specifically deuterated hemins. The results indicate the pattern of unpaired spin delocalization about the porphyrin and lead to the prediction that the heme orientation in HRP-CN will be similar to that in CcP-CN. By analysis of the assigned resonances for CcP and the crystal structure, the proximal histidine rotational orientation alone is shown to be capable of explaining the rhombic perturbation. However, evidence is also presented which suggests that peripheral heme-protein contacts may contribute to the perturbation.

Acknowledgment. We gratefully acknowledge support for this research from several sources: American Heart Association (J.D.S.) and the Sandia-UNM Research Program (SURP)(J. D.S.); the National Institutes of Health (GM 18648 (J.E.E.); HL 22252 (K.M.S.); HL 16087, GM 26226 (G.N.L.)). We also acknowledge the Purdue University Biochemical Magnetic Resonance Laboratory, through which part of this research was supported by the National Institutes of Health, Division of Research Resources RR 01077; and the University of California, Davis, NMR Facility.

Registry No. Cytochrome *c* peroxidase, 9029-53-2; [1,5-$^2H_6$]hemin, 84848-82-8; [1,3-$^2H_6$]hemin, 84848-81-7; [2,4-$^2H_4$]hemin, 84848-80-6; [4-$^2H_3$]hemin, 84848-79-3; [2,4-$^2H_2$]hemin, 82113-45-9; [6,7β-$^2H_4$]hemin, 84848-78-2.

Multinuclear NMR Study of the Solvated Electron in Lithium-Methylamine Solutions

Dolores M. Holton,[†] Peter P. Edwards,*[†] William McFarlane,[‡] and Brian Wood[‡]

Contribution from the University Chemical Laboratory, Cambridge, CB2 1EW, United Kingdom, and the Department of Chemistry, City of London Polytechnic, London, ED3N 2EY, United Kingdom. *Received June 8, 1982*

Abstract: We report a multinuclear NMR study of lithium-methylamine solutions. NMR Knight shift data for solvent (^1H, ^{13}C, ^{14}N) and metal (^6Li, ^7Li) nuclei are reported for concentrations from 2 mol % lithium to saturation at ca. 200 K. The NMR results have been used in conjunction with recent magnetic susceptibility measurements on the title system to provide a precise description of the unpaired-electron spin-density distribution in both the solvated electron, e^-_s, and lithium monomer species, $Li^+_s e^-_s$. For both species, the vast majority of the unpaired-electron spin density resides in the nitrogen fragment of the solvent molecule. As with metal-ammonia solutions, we also find a small, negative spin density in the ^1H 1s orbital. The occupancy of the ^6Li and ^7Li 2s orbital in the electron-cation aggregate species $Li^+_s e^-_s$ corresponds to approximately 0.5% of the lithium free-atom value for a 7 mol % metal solution. We conclude that the excess-electron species in lithium-methylamine solutions resides in a ground-state orbital which is composed of a simple 1s-like orbital for the electron within a solvent cavity, in combination with a set of Rydberg-like orbitals derived from the 3s orbitals of the host solvent matrix.

Introduction

Metal-ammonia solutions have been the subject of considerable attention from both chemists and physicists for almost two centuries.[1-3] In this system, comprehensive optical, conductivity, and magnetic data (among other properties) now exist over something like five orders of magnitude in concentration.[3] With this background it is natural, as Dye has suggested,[4] that in any general description of metal solutions we invariably return to the metal-ammonia system for guidance. However, the study of metal

[†] The University Chemical Laboratory.
[‡] City of London Polytechnic.

(1) (a) "Metal-Ammonia Solutions, Physicochemical Properties", Colloque Weyl I, Lille, 1963; Lepoutre, G., Sienko, M. J., Eds.; W. A. Benjamin: New York, 1964. (b) "Metal-Ammonia Solutions", Colloque Weyl II; Lagowski, J. J., Sienko, M. J., Eds.; Butterworths: London, 1970. (c) "Electrons in Fluids", Colloque Weyl III; Jortner, J., Kestner, N. R., Eds.; Springer-Verlag: Berlin, 1973. (d) Colloque Weyl IV *J. Phys. Chem.* **1975**, *79*, 2789. (e) Colloque Weyl V *Ibid.* **1980**, *84*, 1065.

0002-7863/83/1505-2104$01.50/0